



HAL
open science

Fore-arc basin deformation in the Andaman-Nicobar segment of the Sumatra-Andaman subduction zone: Insight from high-resolution seismic reflection data

Raphaële E. Moeremans, Satish C. Singh

► To cite this version:

Raphaële E. Moeremans, Satish C. Singh. Fore-arc basin deformation in the Andaman-Nicobar segment of the Sumatra-Andaman subduction zone: Insight from high-resolution seismic reflection data. *Tectonics*, 2015, 34, pp.1736-1750. 10.1002/2015TC003901 . insu-03579673

HAL Id: insu-03579673

<https://insu.hal.science/insu-03579673>

Submitted on 18 Feb 2022

HAL is a multi-disciplinary open access archive for the deposit and dissemination of scientific research documents, whether they are published or not. The documents may come from teaching and research institutions in France or abroad, or from public or private research centers.

L'archive ouverte pluridisciplinaire **HAL**, est destinée au dépôt et à la diffusion de documents scientifiques de niveau recherche, publiés ou non, émanant des établissements d'enseignement et de recherche français ou étrangers, des laboratoires publics ou privés.

Copyright



RESEARCH ARTICLE

10.1002/2015TC003901

Key Points:

- Despite obliquity of convergence, the fore arc is dominated by compression
- Slip is strongly partitioned along the Andaman-Nicobar segment of subduction
- Changes in the fore-arc basin are related to phases of opening in Andaman Sea

Correspondence to:

R. E. Moeremans,
moeremans@ipgp.fr

Citation:

Moeremans, R. E., and S. C. Singh (2015), Fore-arc basin deformation in the Andaman-Nicobar segment of the Sumatra-Andaman subduction zone: Insight from high-resolution seismic reflection data, *Tectonics*, 34, 1736–1750, doi:10.1002/2015TC003901.

Received 8 APR 2015

Accepted 19 JUL 2015

Accepted article online 23 JUL 2015

Published online 27 AUG 2015

Fore-arc basin deformation in the Andaman-Nicobar segment of the Sumatra-Andaman subduction zone: Insight from high-resolution seismic reflection data

Raphaële E. Moeremans¹ and Satish C. Singh¹¹Laboratoire de Géosciences Marines, Institut de Physique du Globe de Paris, Paris, France

Abstract The Andaman-Nicobar region is the northernmost segment of the Sumatra-Andaman subduction zone and marks the western boundary of the Andaman Sea, which is a complex active back-arc extensional basin. We present the interpretation of a new set of deep seismic reflection data acquired across the Andaman-Nicobar fore-arc basin, from 8°N to 11°N, in order to better understand its structure and evolution, focusing on (1) how obliquity of convergence affects deformation in the fore arc, (2) the nature and role of the Diligent Fault (DF), and (3) the Eastern Margin Fault (EMF). Despite the obliquity of convergence, back thrusting and compression seem to dominate the Andaman-Nicobar fore-arc basin deformation. The DF is primarily a back thrust and corresponds to the Mentawai and West Andaman Fault systems farther in the south, along Sumatra. The DF is expressed in the fore-arc basin as a series of mostly landward verging folds and faults, deforming the early to late Miocene sediments. The DF seems to root from the boundary between the accretionary complex and the continental backstop, where it meets the EMF. The EMF marks the western boundary of the fore-arc basin; it is associated with subsidence and is expressed as a deep piggyback basin, containing recent Pliocene to Pleistocene sediments. The eastern edge of the fore-arc basin is the Invisible Bank (IB), which is thought to be tilted and uplifted continental crust. Subsidence along the EMF and uplift and tilting of the IB seem to be related to different opening phases in the Andaman Sea.

1. Introduction

Fore-arc basins are important features of subduction margins. They form structurally due to a variety of subduction zone processes and fill up with sediments in response to a combination of tectonic processes and sediment supply [Dickinson and Seely, 1979]. Their evolution is thus recorded in the depositional sequences as a series of subsidence and uplift events, directly associated with subduction processes, over millions of years [Laursen et al., 2002; Berglar et al., 2008; Ryan et al., 2012]. The basin evolution can thus provide a history of local as well as regional tectonics along the margin. The Andaman-Nicobar fore-arc basin contains 3 to 5 km of sediment fill of Cenozoic age [e.g., Pal et al., 2003], recording the evolution of the basin over the last ~60 Ma. Constraining the evolution of this basin can help shed light onto present-day deformation processes along this segment of the subduction zone, where subduction is highly oblique and little data are available.

Additionally, fore-arc basins are thought to play a role in the seismic cycle as well as during large earthquake ruptures. Recent studies [e.g., Fuller et al., 2006] have observed a relationship between fore-arc basins and slip during subduction earthquakes and thus structures in the overriding plate and seismic coupling at the plate interface. Maximum slip during large subduction earthquakes has been shown to preferentially occur where sedimentary basins are present to stabilize the wedge. In particular, Marone [1998] argues that fault zones become more prone to seismic slip as the rate of loading on the fault zone increases. Better understanding of seismic rupture processes is crucial along this segment of the Sumatra-Andaman subduction zone, as its entirety ruptured during the December 2004 $M_w \sim 9.3$ event [e.g., Lay et al., 2005], and high near-trench slips were recorded in the fore-arc area during this event [Rhie et al., 2007; Chlieh et al., 2007].

The objective of this paper is to understand the relation between oblique subduction and fore-arc basin evolution by investigating the deposited sedimentary sequences and their relationship with the major tectonic features in the area, in order to shed light onto present-day tectonic processes. Furthermore, this study would allow for a better understanding of fore-arc morphology, deformation, and tectonic evolution in a system of highly oblique subduction. The Andaman-Nicobar segment of the Sumatra-Andaman subduction zone has undergone changing tectonic regimes through time and presently constitutes an end-member of the

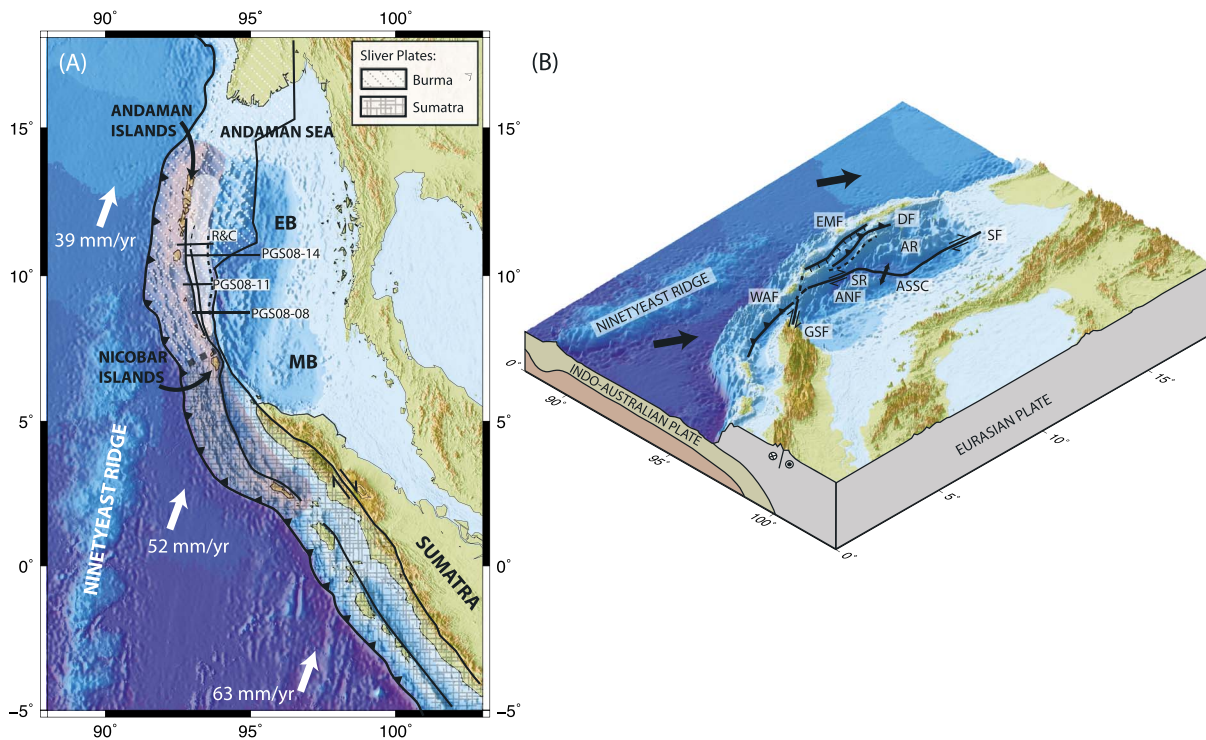


Figure 1. (a) Bathymetric map of the study area, showing the location of the seismic reflection profiles across the fore arc of the Andaman Sea. Black arrows indicate the rates and direction of convergence between the Indo-Australian and Eurasian Plates. The red shaded area is the rupture area of the December 2004 earthquake. The white shaded area marks the position of the Andaman-Nicobar fore-arc basin. (b) Three-dimensional view of the Andaman Sea Basin, showing the major geological features. ANF = Andaman-Nicobar Fault; AR = Alcock Rise; ASSC = Andaman Sea Spreading Center; CB = Central Basin; DF = Diligent Fault; EMF = Eastern Margin Fault; GSF = Great Sumatra Fault; MB = Mergui Basin; SF = Sagaing Fault; SR = Sewell Rise; and WAF = West Andaman Fault.

spatiotemporal variability along the subduction system. Obliquity has increased through time, from orthogonal to nearly trench-parallel subduction and back-arc rifting, offering a unique opportunity to study the development of fore-arc basins through contrasting kinematic episodes. The major questions that are addressed here are (1) how oblique subduction affects fore-arc basin evolution and (2) how rifting in a back-arc basin affects fore-arc basin development. The Andaman-Nicobar fore-arc basin is an ideal setting to address these questions because of its geological history, its close proximity to sedimentary sources from both the outer-arc high and magmatic arc, its position in a highly seismic environment, and the high quality of this newly acquired data set.

The results are related to and compared with basin evolution and structure in Java and southern Sumatra, where the fore-arc basin is more extensively studied and understood, and the activity of the major tectonic features is better constrained [Schlüter *et al.*, 2002; Mukti *et al.*, 2012]. Here we will mainly focus on the fore-arc basin, east of the Andaman-Nicobar Islands; the study of the deformation front and accretionary wedge is presented in Moeremans *et al.* [2014] and will not be discussed here.

2. Tectonic Setting

2.1. Oblique Subduction

The Andaman-Sumatra subduction zone extends over more than 3000 km and is the result of the convergence between the downgoing Indo-Australian Plate and the overriding Eurasian Plate. Present-day convergence at the Sumatra-Andaman subduction is a classical example of oblique subduction, with convergence rates varying from 63 mm/yr in South Sumatra to 52 mm/yr in northern Sumatra [Prawirodirdjo and Bock, 2004] and 43 mm/yr off of the Andaman Islands [Gahalaut *et al.*, 2006]. The Andaman-Nicobar segment of the Sumatra-Andaman subduction is located at the northern end of the subduction system (Figure 1a), where subduction is highly oblique, occurring at an angle of $\sim 11^\circ$ from trench parallel. Geodetic data indicate that it occurs at rates between ~ 14 and 34 mm/yr north of 8°N [Paul *et al.*, 2001; Gahalaut *et al.*, 2006].

As a result of obliquity, the slip related to the convergence between the two plates is partitioned into a trench-perpendicular component and a trench-parallel component, which is mostly accommodated along the Sumatra Fault, which acts as a strike-slip sliver fault [e.g., *Fitch*, 1972; *McCaffrey*, 1992], and a sliver plate, the Burma Plate [*Curry et al.*, 1979] (Figure 1a), is formed between the trench and the complex right-lateral strike-slip sliver fault. The strike-slip fault rate increases with the obliquity of plate convergence. Estimates of the rates in Myanmar by *Vigny et al.* [2003] are of total of 35 mm/yr, with < 20 mm/yr along the Sagaing Fault (SF) itself. *Curry* [2005] estimates of N-S motion in Central Andaman Basin are of 27 mm/yr; *Sieh and Natawidjaja* [2000] and *Genrich et al.* [2000] estimated rates of ~25 mm/yr at NW Sumatra and 10–20 at SE Sumatra, respectively. In the Andaman Sea, the trench-parallel motion of convergence is accommodated along the Andaman-Nicobar sliver fault (ANF) [*Singh et al.*, 2013]. The ANF joins the Andaman Sea Spreading Center (ASSC) and then connects with the Sagaing Fault (SF) in Myanmar [*Vigny et al.*, 2003], farther north (Figure 1b).

2.2. Evolution of the Subduction System and the Andaman Sea

Subduction along the Sunda margin began during the Late Cretaceous period, after the early breakup of Gondwana Land [*Curry and Moore*, 1974; *Karig et al.*, 1979; *Moore et al.*, 1982]. The collision between greater India and Eurasia during the late Paleocene, around 59 Ma ago, started a clockwise rotation and bending of the northwestern Sunda subduction, increasing the obliquity of convergence [*Klootwijk et al.*, 1992; *Curry*, 2005]. The initial sliver strike-slip fault probably started in the middle to late Eocene, extending through the outer-arc ridge offshore Sumatra and connecting with the present-day Sagaing Fault in the north through the Central Andaman Basin [*Curry*, 2005]. Opening in the Andaman Sea began in the Miocene, as a consequence of the collision between India and Eurasia, followed by subsequent extrusion activity, clockwise rotation of continental blocks, and crustal motion along strike-slip faults [e.g., *Tapponnier et al.*, 1982]. Extensional basins are suggested to have opened in sequence, starting with the Mergui Basin ~ 32 Ma, the Alcock and Sewell Rises ~ 23 Ma, the East Basin ~ 15 Ma, and the Central Andaman Basin ~ 4 Ma [*Curry*, 2005].

2.3. The Andaman-Nicobar Segment

The Andaman Sea basin spans 1200 km in length, from Burma and its Irrawaddy delta to northern Sumatra, and 650 km in width, from the west coast of the Malay Peninsula to the Andaman-Nicobar Islands, which are the subaerial parts of the Andaman-Nicobar Ridge. The eastern boundary of the basin is the Malayan continental shelf. The western boundary of the Andaman Basin is expressed as the Andaman-Nicobar Ridge, which was suggested to consist of Upper Cretaceous ophiolite slices overlain by Paleocene to Miocene sediments [*Rodolfo*, 1969]. Opening in the Andaman Basin started in late Miocene and is believed to have occurred in distinct phases [e.g., *Curry*, 2005; *Khan and Chakraborty*, 2005; *Morley and Alvey*, 2015].

The Andaman-Nicobar fore-arc geomorphology is characterized by 85 to 150 km wide accretionary wedge, a shallow fore-arc high lying at 300 to 1500 m of water depth, and a fore-arc basin filled with 3 to 5 km of sediments, bounded in the west by the Eastern Margin Fault (EMF) and in the east by the tilted and uplifted Invisible Bank (Figure 2). The sedimentary cover on the subducting plate is very thick due to the Bengal Fan sediments, which have been accreted into the wedge. The sedimentary cover of the Bengal Fan thins over the NinetyEast Ridge (NER) [*Moeremans et al.*, 2014], which seems to indent the trench at between ~6 and 9°N. The accretionary wedge has emerged in some places along the margin, creating a chain of fore-arc high, including the Andaman and Nicobar Islands, but extending to Enggano Island off southern Sumatra.

The major faulting structures within the fore-arc area of this segment of the margin consist of the Andaman-Nicobar Fault (ANF), the Diligent Fault (DF), and the Eastern Margin Fault (EMF) (Figures 1b and 2) [*Curry*, 2005; *Cochran*, 2010; *Singh et al.*, 2013]. The ANF, which was established as the northward continuation of the sliver Great Sumatra Fault (GSF), merges with the Andaman Sea Spreading Center (ASSC) at 11°N. A back thrust system, the DF, was imaged as deforming the thick fore-arc basin sediments as a series of anticlinal ridges; this back thrust system was suggested to be analogous to the West Andaman Fault (WAF) and the Mentawai (MFZ). The EMF, which marks the western boundary of the fore-arc basin, has been interpreted as accommodating subsidence [*Cochran*, 2010]. Finally, it was proposed that the basement of the Andaman-Nicobar fore-arc basin is Malayan continental crust, similarly to the Sumatran fore-arc basement [*Singh et al.*, 2013]. The sliver ANF lies to the east of the IB and marks the boundary between continental crust underlying the fore-arc basin and crust accreted at the Andaman Sea Spreading Center (Figure 2).

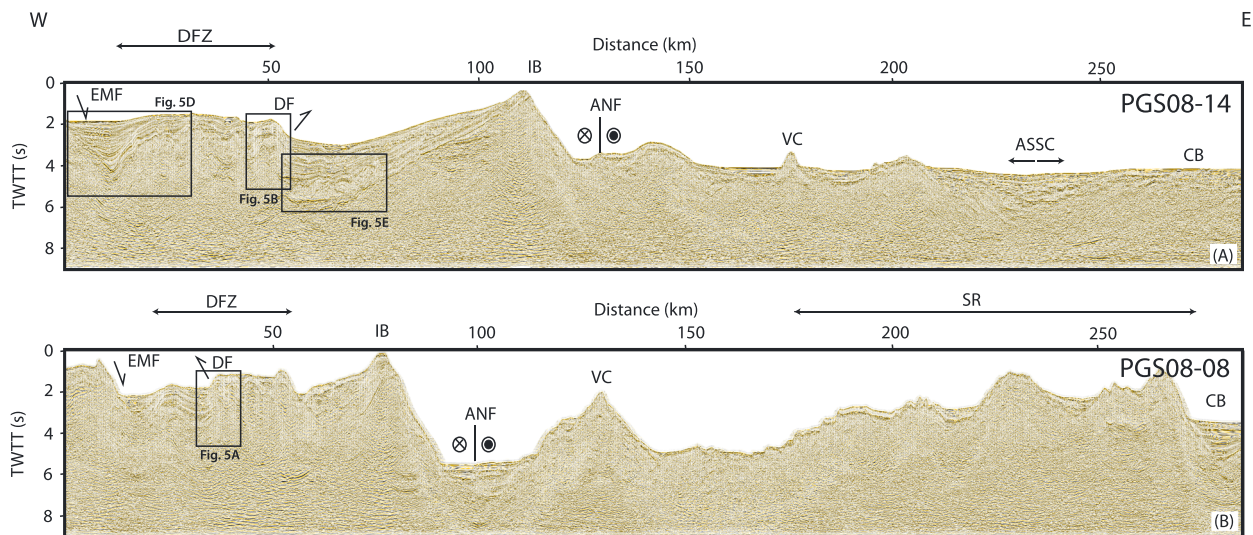


Figure 2. Two long seismic reflection profiles, showing the fore-arc structure from the fore-arc basin to the Andaman Sea Spreading Center. Black boxes indicate areas that are shown in Figure 5. (a) PGS08-14. (b) PGS08-08. ANFB = Andaman-Nicobar Fault Basin; ANF = Andaman-Nicobar Fault; ASSC = Andaman Sea Spreading Center; DF = Diligent Fault; DFZ = Diligent Fault Zone; EMF = Eastern Margin Fault; IB = Invisible Bank; SR = Sewell Rise; and VC = Volcanic Cone.

2.4. Stratigraphy

The main sediment source for the Andaman Basin is the Irrawaddy River, with an annual discharge of 265×10^6 tons of silty clay [Rodolfo, 1969]. Density flows are channeled by submarine canyons. The fore-arc basin contains a 3–3.5 km thick sediment fill (Figure 3) of Cenozoic age, recording the evolution of the Andaman-Nicobar fore arc over the past ~ 60 Ma.

The stratigraphy along the Andaman-Nicobar segment of the margin has been investigated in previous studies, using sediment cores, seafloor dredges, and formations exposed on the islands [Rodolfo, 1969; Roy and Chopra, 1987; Chakraborty and Pal, 2001; Pal et al., 2003]. In this section, the stratigraphy of the Andaman-Nicobar basin will be considered from west to east. Three major sedimentary groups are present in the Andaman-Nicobar fore arc [e.g., Rodolfo, 1969; Pal et al., 2003; Curray, 2005].

The oldest group, the Eocene Mithakhari Group, consists of pelagic trench sediments and coarser ophiolite fragments. It is 1.4 km thick and is found in the accretionary prism. The Andaman-Nicobar accretionary prism is composed of dismembered Cretaceous ophiolite slices that were uplifted and emplaced by a series of seaward verging thrusts, interbedded with Eocene trench slope sediments, with progressively younger rocks to the west [Pal et al., 2003; Curray, 2005]. The ophiolites were formed at the Tethys Sea that was between Asia and India. These rocks have been strongly folded and deformed by the seaward verging thrust faults and are overlain by flat-lying and undeformed Miocene to recent reef-derived clastics [Rodolfo, 1969]. Similarly, the Paleocene rocks found on Nias Island, off northern Sumatra, are folded and faulted by seaward verging thrusts and are overlain by Pliocene and younger flat-lying deposits [Moore et al., 1980]. In addition, Nias also has pre-Miocene mélangé overlain by Miocene and younger strongly deformed trench slope deposits [Moore et al., 1980].

The Andaman-Nicobar Islands are the subaerial expression of the Andaman-Nicobar accretionary prism. These islands are thought to be a northerly continuation of the Mentawai Islands in the south. The Paleogene Andaman-Nicobar Ridge (ANR) stood above sea level for the first time following uplift and compression in the Oligocene and late Miocene [Rodolfo, 1969]. Subsequently, N-S normal and E-W strike-slip faults resulted in the development of a fore-arc basin with deposition of Oligocene and Mio-Pliocene sediments [Pal et al., 2003]. Continental crust from the Malay Peninsula was rifted and thinned to form the Mergui Basin in the east [Curray, 2005].

Two deposits are found in the fore arc: the Andaman Flysch Group (AFG) and the Archipelago Group (AG). The AFG is of upper Eocene-Oligocene age. It is ~ 3 km thick, composed of three different lithofacies, and overlies and onlaps the Mithakhari Group. The Andaman Flysch is thought to have developed in a fore-arc

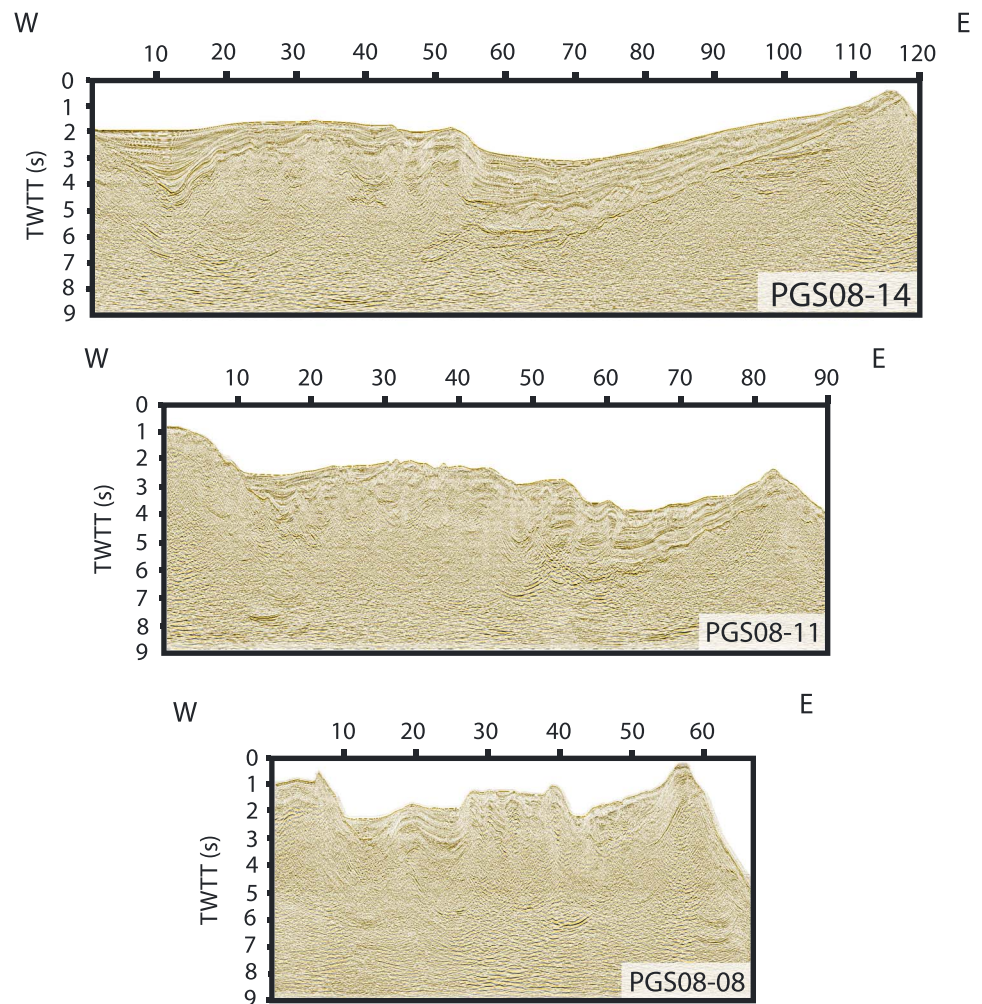


Figure 3. Uninterpreted seismic reflection profiles (top) PGS08-08, (middle) PSG08-11, and (bottom) PGS08-14 across the Andaman-Nicobar fore-arc basin.

setting adjacent to the accretionary wedge, as longitudinal fan resulting from sediment supply parallel to the basin axis, and occasionally transversely from the basin margin. Fore-arc sedimentation often occurs around the same time as uplift of the accretionary complex and later stage deformation in the margin. Sediments in the fore-arc basin are thus younger than the accretionary prism material. The AFG is unconformably overlain by the AG, which are Miocene to Pliocene aged sediments, thought to have been deposited in an outer shelf to open marine environment [Chakraborty and Pal, 2001]. The AG is composed of two major assemblages of turbidites. In comparison with the AFG and the AG, the Mithakhari Group shows complex deformation, with highly variable bedding orientations [Pal et al., 2003].

2.5. Seismicity

The Andaman-Nicobar region is an area of high seismic risk. The trench portion of this segment ruptured entirely during the December 2004 event ($M_w \sim 9.3$), one of the largest events ever recorded. The rupture initiated at a depth between 30 and 40 km near Simeulue Island and propagated over a length of 1300 km and width of 150 km up to the northern Andaman Islands [Lay et al., 2005; Chlieh et al., 2007] (Figure 1a). The average slip was 12 to 15 m [Stein and Okal, 2005], with maximum slips of more than 20 m near the trench [Rhie et al., 2007] and around 10 m in the Andaman-Nicobar fore arc [Rhie et al., 2007; Chlieh et al., 2007]. Historical events along the plate boundary in the Andaman region occurred beneath the Nicobar Islands in 1847 ($M_w > 7.5$) and 1881 ($M_w 7.9$), and near the Andaman Islands ($M_w 7.9$) in 1941, but occurred mostly to the east and at greater depths than the December 2004 event [Bilham et al., 2005].

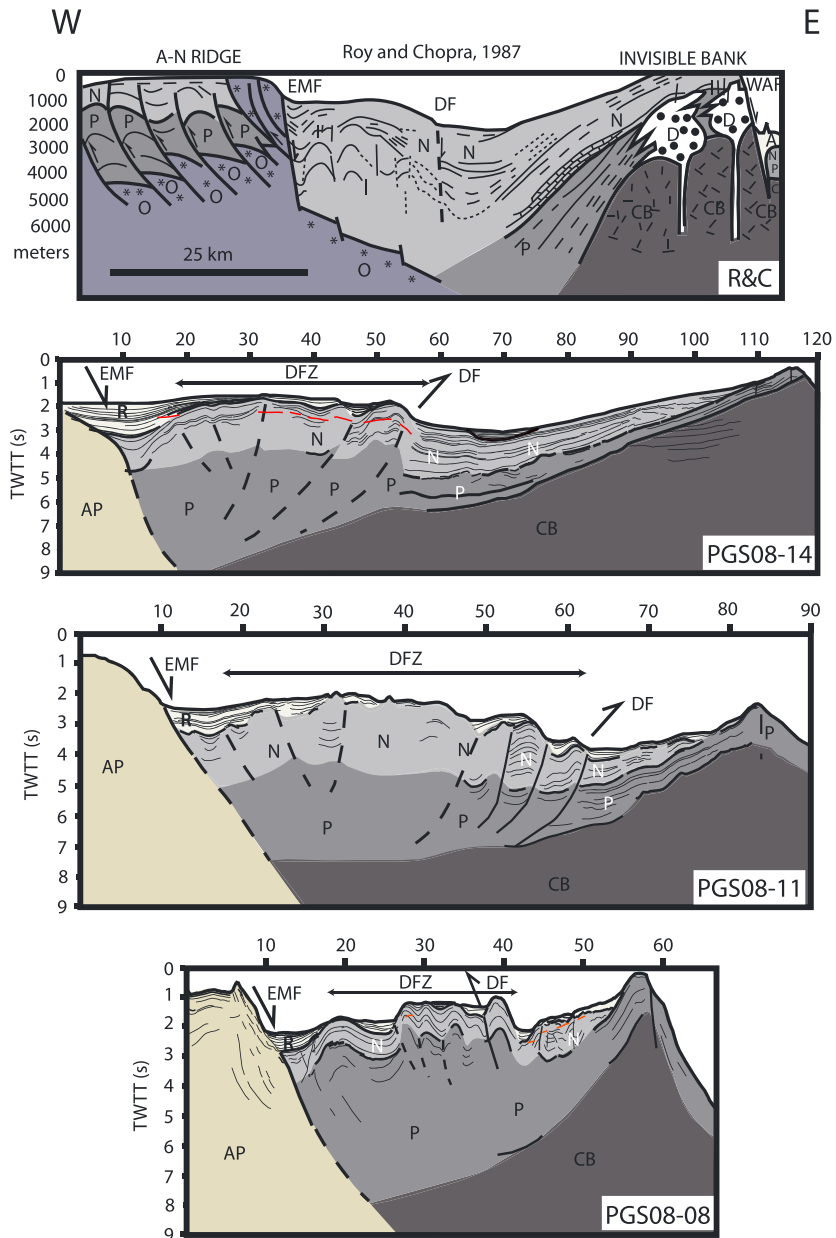


Figure 4. Interpreted seismic reflection profiles from (a) Roy and Chopra [1987], (b) PGS08-08, (c) PGS08-11, and (d) PGS08-14 across the Andaman-Nicobar fore-arc basin. A = Recent andesitic flows; AP = accretionary prism; CB = Continental Basement; D = pre-Miocene diabase; N = Neogene Unit 2; O = oceanic basement; P = Cretaceous-Oligocene Unit 1; and R = Recent Unit 3. BSRs are marked in red.

Earthquake hypocenters from the Andaman Islands and Andaman Sea indicate a Benioff zone dipping 45–55° toward the east and record epicenters at 200 km focal depth [Pesicek et al., 2010]. Beneath the accretionary prism and the Andaman-Nicobar Ridge, the slab dips at a shallow angle and then turns sharply down beneath the fore-arc basin axis [Cochran, 2010].

3. Data Acquisition and Processing

We use three high-resolution seismic reflection profiles acquired by Petroleum GeoServices (PGS) in 2008 (Figures 1a and 3), using an 8 km long streamer towed at 7.5 m water depth and an array of air guns with a total volume of 81.93 L towed at 6 m. The shot interval was 25 m, and the record length was 9 s. The data

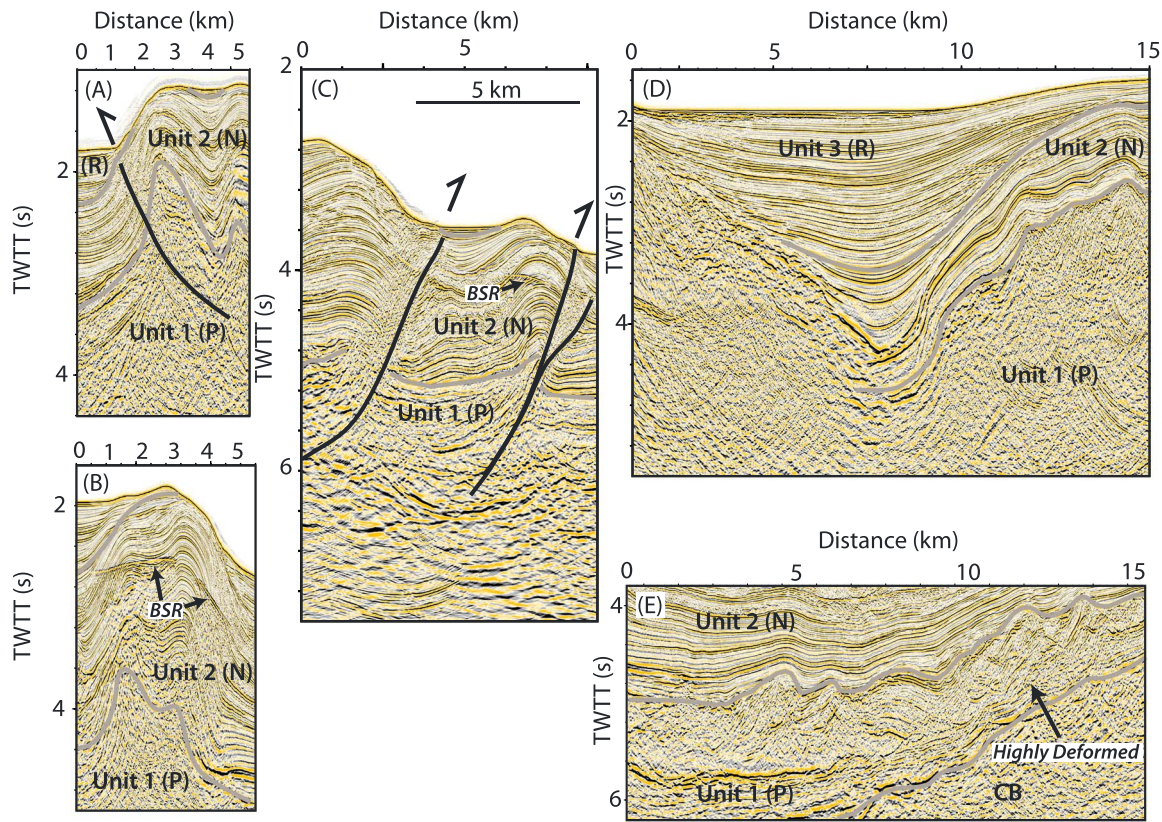


Figure 5. Blow ups from profiles PGS08-08, PGS08-11, and PGS08-14. Locations of these blow ups within the long profiles are shown in Figure 2. (a) Seaward verging thrust in PGS08-08, (b) landward verging back thrust in PGS08-14, (c) landward back thrust in PGS08-11, (d) EMF Basin in PGS08-14, and (e) landslide in PGS08-14.

were processed by PGS up to prestack time migration, using conventional processing techniques. All profiles were acquired orthogonally to the trench and are thus oriented in an E-W direction. They cover the fore-arc basin, from the fore-arc high on the seaward end to the Invisible Bank on the landward end, between the Nicobar Islands at 8°N and the Andaman Sea Spreading Center at 11°N.

4. Seismic Profile Interpretation

Figure 2 shows two representative profiles covering the whole of the fore-arc system in the Andaman Sea, from the fore-arc high to the back-arc basin. In Figure 3, we show three uninterpreted profiles covering the fore-arc basin in the north, center, and south of our study area, and in Figure 4, we show the interpretations of these seismic reflection profiles.

Profile PGS08-14 (Figure 2a) is located in the northern end of the study area. It extends from the fore-arc high in the east to the Central Basin (CB) in the west. The fore-arc basin is ~110 km wide, from the EMF basin (also shown in Figure 5d) to the IB, which is < 500 m below sea level. The EMF basin, which results from subsidence along the EMF, contains > 2 s two-way travel time (TWTT) of flat-lying sediment, which overlap onto a 40 km wide series of back thrusts, the DFZ. The DF is the easternmost back thrust (blown up in Figure 5b). Bottom-simulating reflectors (BSRs) are observed both in the sediments on the eastern side of the EMF basin and over the DFZ ridges (Figures 2a, 5b, and 5c). The fore-arc basin contains ~3.5 s TWTT of sediment, which are tilted and uplifted. The fore-arc basin sediments are highly tectonically deformed at the bottom of the basin (Figure 5e). The ANF is located ~15 km east of the IB, at 4 s TWTT, and is expressed as a small upwarp of the seafloor on the landward side (Figure 2a), with thin offset sediments on either side. Two basement highs, at 140 and 200 km respectively, define the extremities of a small basin filled with ~1 s TWTT of sediment. A volcanic cone is visible at 175 km, at the center of the basin. The profile then crosses the thickly

sedimented ASSC, which is covered in 2 s TWTT of sediment at its axis and marked by a series of outward tilted normal fault blocks on its flanks. At the eastward end of the profile, the CB is covered by ~1 s TWTT of sediment.

Profile PGS08-08 (Figure 2b) is located at the southern end of our study area. It also extends from the fore-arc high to the CB. Here the fore-arc basin is much more narrow, spanning only 75 km in width. It is also bounded in the west by the EMF and in the east by the IB. The DFZ is dominated by seaward verging back thrusts (Figure 5a) and smaller-amplitude folds. The fore-arc basin is traversed by a prominent BSR (Figure 2b). The IB is much shallower here, reaching up to ~100 m below sea level. The seafloor to the east of the IB is at 5.5 s TWTT (versus 3.5 s TWTT in PGS08-14). The ANF trace is much clearer in this profile, at 100 km, and can be followed down to 7 s TWTT. The ANF basin is more sedimented in this profile, with ~1 s TWTT of sediments offset by the fault. A large volcanic cone (VC) (~25 km wide and 3 km high) is seen directly east of the ANF basin. To the east of this VC, the oceanic seafloor is not sedimented until km 175, where en échelon crustal blocks, progressively covered in 0.5 s TWTT of sediment, mark the western flank of the Sewell Rise (SR). The SR extends for about 100 km in width, until the CB.

Several major tectonic structures have thus been identified within the fore-arc basin: (1) the Eastern Margin Fault (EMF), which marks the western boundary of the fore-arc basin and is associated with a small basin filled with more recent sediments (Figure 5d); (2) the DF system, which is expressed as a series of mostly landward vergent back thrusts and folds (Figures 5a–5c); and (3) a normal fault cutting through the IB, on its eastern flank (Figures 3 and 4). BSRs are abundant within the sediments of the fore-arc basin, particularly in the sediments uplifted by the DF.

4.1. Stratigraphic Units and Major Tectonic Features

We identify three major stratigraphic units in the Andaman-Nicobar fore-arc basins and interpret these and other structures present in the fore-arc basin in light of both previous studies conducted in the Andaman-Nicobar region [Rodolfo, 1969; Chakraborty and Pal, 2001; Pal et al., 2003; Curray, 2005] and studies that were carried out in the fore-arc basin of southern Sumatra [e.g., Schlüter et al., 2002; Mukti et al., 2012]. We define these major seismic stratigraphic units based on their seismic characteristics and unconformities between them (Figure 4). We start by characterizing the main identified units and describe variations in our profile interpretations from south to north. We then roughly constrain their ages based on major known tectonic events and previous stratigraphic studies discussed above. Correlations between the stratigraphy from previous studies and the seismic reflection profiles used in this study may give rise to some uncertainty in the results described below. The deepest part of the fore-arc basin, located directly east of the DF, can be divided into three mega-sequences. The ages assigned to these units follow the profile interpretation of Roy and Chopra [1987], which is shown in Figure 4a (location marked as R&C in Figure 1). Unit 1 (P in Figure 4) consists of seaward dipping reflectors characterized by high amplitudes. These reflectors are interpreted as the oldest sedimentary unit of the fore-arc basin, which was deposited directly on top of the basement (CB in Figure 4). Unit 2 (N in Figure 4) onlaps onto Unit 1, indicating that turbidite sediments were deposited horizontally onto a sloping surface. It is characterized by generally lower amplitude reflections. It is also seaward dipping and likely corresponds to Miocene-Pliocene sediments, but the upper part of Unit 2 could be as young as early Pleistocene. Unit 3 (R in Figure 4) consists of flat-lying reflectors onlapping onto Unit 2 sediments and corresponds to Recent deposits. Both Units 1 and 2 have been uplifted and tilted seaward in the east and deformed by the back thrust in the west. Unit 3 fills lows in the fore arc with flat-lying relatively undisturbed sediments. We will discuss these different units below, but first, we will discuss the nature of the basement.

4.1.1. Basement

The top of the basement of the fore-arc basin is interpreted as high-amplitude reflectors that are dipping westward. Its eastward end, the Invisible Bank, can be as shallow as a few meters water depth (profiles PGS08-14 and PGS08-08, Figures 3 and 4) at both along-strike extremities of our study area. The high amplitude of these reflections indicates a sharp contrast (increase) in the velocity across this boundary. In profiles PGS08-14 and PGS08-11, relief of 500–750 m is evident along the top of the basement horizon. Below these high-amplitude reflections that represent the top of the basement, returned acoustic energy is sparse. In some profiles, however, further reflections are visible, which might be due to old sedimentary layering within the crustal material [Singh et al., 2013]. In the northern profiles (PGS08-14) its topography is a bit rough and some discontinuous high-amplitude reflections occur locally below the top of the basement reflection (PGS08-14) (Figure 3).

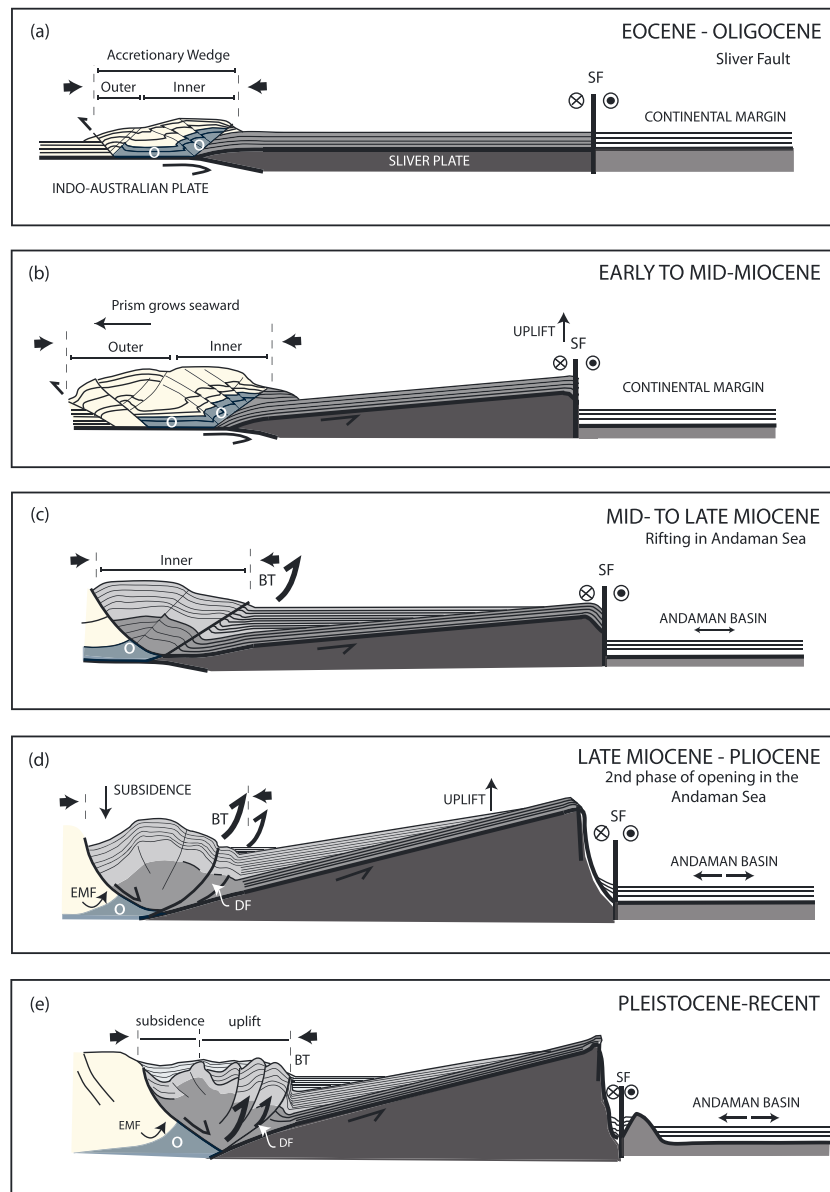


Figure 6. Schematic diagram showing the tectosedimentary events during the evolution of the Andaman-Nicobar fore-arc region. O = ophiolites; BT = Backthrust; and SF = Sliver Fault.

4.1.2. Unit 1

Unit 1, annotated as P (Paleogene) in Figure 4, appears as subparallel smooth reflections that were deposited conformably over the fore-arc basement. This unit also dips westward and must have been deposited prior to uplift and subsequently tilted and uplifted along with the basement (Figures 3 and 4). It is composed of two to three depositional subunits that are separated by reflections of high-amplitude and/or depositional onlap of the top reflections onto the lower reflections. This unit was deposited as flat-lying beds, and we thus postulate that the IB had not been uplifted yet at the time of deposition (Figure 6a). Deposition of this unit should therefore date from pre-Miocene times. Some slumping and landsliding or syntectonic deformation can be seen in this unit (e.g., PGS08-14 in Figure 5e). These sediments could also be shale moving about.

4.1.3. Unit 2

Unit 2, annotated as N (Neogene) in Figure 4, can also be divided into two subunits. Onlap and deformation of Unit 2 (e.g., in PGS08-11) indicate that the deformation within the basement resumed for a little bit during deposition of Unit 2. In contrast with Unit 1, which was deposited conformably over the top of the basement

prior to uplift and to have been tilted and uplifted along with it after deposition, Unit 2 was deposited after some uplift of the basement had already taken place (Figure 6b). Syntectonic deformation can be seen in this Unit 2 as well. A second episode of uplift occurred during the deposition of this unit, corresponding to the second subunit.

4.1.4. Unit 3

This unit, annotated as R (Recent) in Figure 4, is the most recently deposited unit. It is characterized by flat-lying reflectors (Figures 3 and 4). The sediments of this unit were deposited after the major uplift phase. The unit is only slightly deformed and fills the lows within the basin, on either side of the DF (Figure 6e). A significant portion of the subsidence along the EMF had occurred prior to the deposition of this unit, particularly in the north of the study area. Unit 3 fills the lows between the thrust sheets formed by the DFZ in the northern profiles (Figure 3, top), but it is less thick and does not mask the seafloor relief in the southern profiles (Figure 3, bottom).

4.1.5. Invisible Bank

The Invisible Bank (IB) is shallowest at both extremities of the basin (near sea level in PGS08-08 and PGS08-14; Figures 3 and 4). It is a cuesta formed by the sliver fault (Figure 6b), which is consistent with the fact that it extends all along the Andaman-Nicobar segment, beyond our study area. Invisible Bank is approximately 300 km long and 5 km wide. Miocene limestones were dredged on the eastern flank of the IB at 1000 m depth [Rodolfo, 1969]. Roy and Chopra [1987] report that drilling near the crest of the IB encountered thick lava flows below 1100 m of middle Miocene sedimentary rocks, which had been previously recovered, dated, and characterized from dredging samples (e.g., Dredge 12 (~11.5°N) with rocks ~17 Ma uplifted ~400 m since deposition or Dredge 13 (~12°N) with ~6 Ma rocks uplifted more than 500 m [Rodolfo, 1969]). Curray [2005] suggests that the sliver fault, which he called WAF (cf. Roy and Chopra profile in Figure 4), formed the cuesta within the last 6 Ma. The seismic reflection profiles used here indicate otherwise because Unit 2 (Miocene) onlaps onto Unit 1, suggesting that some uplift had occurred prior to the deposition of Unit 2 (unless Unit 2 is only 6 Ma, but this is unlikely given sedimentation rates of 50 m/Myr in the Pleistocene and 130 m/Myr in the late Miocene [Flores et al., 2014]). Furthermore, the IB is cut by a steep fault (Figures 3 and 4; WAF in Roy and Chopra [1987]), which is especially prominent in the southern profiles (between PGS08-08 and PGS08-11) but is visible up to PGS08-14. This fault could have been the sliver fault prior to the ANF, similarly to the MFZ and GSF, to the south. Indeed, Curray [2005] had suggested that faulting moved onshore from the MFZ to the GSF, in Sumatra.

4.1.6. Diligent Fault

The DF creates a NE trending structural high, which forms a boundary between the basinal plain and the EMF basin. It is thought to have formed since the pre-Miocene, maybe the middle Eocene (Figures 6a and 6b). The fault zone, which we define as the folded sequence of ridges bounded by the back thrust faults, is 20–40 km wide. The width of the fault zone increases northward (Figures 3 and 4). It is narrowest in the south of the study area, to the east of the Nicobar Islands. It progressively widens and reaches a maximum in profile PGS08-14. The width of individual folds is 2 to 5 km. The width and spacing of individual folds increase northward. The Diligent Fault Zone (DFZ) is biverging with landward vergence dominating in profiles PGS08-11 to PGS08-14 and more mixed vergence in profiles PGS08-08 to PGS08-11. The imbricated back thrusts formed a structural high in the inner wedge, involving the sediments of Units 1 and 2. The imbricated back thrusts may have developed prior to the deposition of Unit 2, i.e., during the Miocene. Possible landslides (Figures 3 (top) and 5e) are observed within the fore-arc basin and at the base of the DF anticlines and could indicate activity on the DF. Mass wasting was also suggested to have taken place in the MFZ [Singh et al., 2010].

Based on these observations of the back thrust system, the Diligent Fault Zone evolution in the Andaman fore-arc basin seems to be very similar to that of the Mentawai Fault Zone. The DF had been previously interpreted as strike slip [Curray, 2005; Cochran, 2010] in the same way the WAF [e.g., Martin et al., 2014] and MFZ [e.g., Diament et al., 1992] had previously been interpreted as strike slips, but here we observe mainly thrusting. While the thrust faults of the DFZ in the northern part of our study area are dominantly landward (eastward) verging, the structure of the DFZ becomes more complex toward the south, directly north of the Nicobar Islands, with mixed thrust vergence and a high variability in the fold amplitudes. We will discuss this complex deformation pattern in section 5.

4.1.7. Eastern Margin Fault

We interpret the EMF to be less active, as no clear fault trace can be identified in the seismic reflection profiles (Figures 3 and 4), but it shows some normal components and is associated with a narrow basin that is up to

3 km deep in profile PGS08-10 (Figures 3 and 4). It may be associated with large-scale westward tilting of the fore-arc basement [Singh *et al.*, 2013] and uplift of the IB, thus possibly predating the DF. The EMF had also been interpreted as a down-to-the-east normal fault between 8°30'N and 11°N by Cochran [2010]. Although it appears that a significant amount of subsidence had occurred prior to deposition of Unit 3 and it does not seem to be presently active, Cochran [2010] had suggested that thickening of the sediments toward the center of the basin indicated continuing subsidence along this fault.

Onlap of the reflectors of Unit 3 onto the top of the underlying accretionary wedge sediments indicates that the piggyback depressions in the fore-arc high formed prior to the deposition of Unit 3, that is, during the Miocene-Pliocene (Figures 6c and 6d). Similar observations in the Mentawai [Mukti *et al.*, 2012], southeast of Enggano and south of western Java [Schlüter *et al.*, 2002], indicate that similar deformation patterns have affected a large region of the South Sumatran fore arc.

4.2. South to North Variations

The width of the fore-arc basin increases significantly northward, but the basin is deeper in the south (Figures 3 and 4). Its width increases from 50 km on profile PGS08-08 to 100 km on profile PGS08-14, but the maximum sediment thickness decreases from 5 s TWTT (~6 km with a *P* wave velocity of 2500 m/s in sediment) on profile PGS08-08 to 3 s TWTT depth on profile PGS08-14. The folds are narrower and the thrust faults steeper in the south. Subsidence along the EMF is greater in the north of the study area.

The structure of the fore-arc basin changes around PGS08-11. The northern profiles display “simpler” deformation patterns with the DFZ characterized by a sequence of prominent landward vergent (eastward) back thrusts with smaller-scale seaward verging (westward) back thrusts under the EMF basin and clearer boundaries between the sedimentary units. The southern profiles (PGS08-08 to PGS08-11), on the other hand, exhibit mixed vergence within the DFZ, with large-amplitude variations between the folds, and boundaries between the sedimentary units are less obvious.

5. Discussion

The relationships between the depositional units and the main tectonic features present in the fore-arc basin allow us to better constrain its evolution and determine a relative sequence of tectonic events (Figures 6 and 7). Age constraints from previously described studies are used to complement this sequence of tectonic events, but there could be some uncertainties. Unit 1 was deposited flat on the basement (Figure 6a) and then uplifted and tilted (Figure 6b). The DF may have initiated around the same time or shortly after. Unit 2 was deposited on top of Unit 1, after the first phase of uplift (Figure 6c). Uplift may have continued with a second phase during deposition of Unit 2 (Figure 6d). Most of the folding and faulting associated with back thrusting occurred concurrently with the deposition of Unit 2. Subsidence along the EMF started simultaneously with the first uplift phase or shortly after the initiation of the back thrust. Folding continued throughout sedimentation, as indicated by downwarping and minor faulting of the sediments at the fold hinges. Unit 3 was deposited after all major tectonic features in the fore-arc basin waned in activity (Figure 6e), although subsidence along the EMF may have been ongoing.

We compare the units identified in our seismic reflection profiles and previous studies in the Andaman fore-arc basin [Rodolfo, 1969; Pal *et al.*, 2003; Curray, 2005] to get approximate ages for the sedimentary units and thus time constraints for the tectonic events. Figure 6 summarizes schematically the major events of the fore-arc basin formation, as resolved by our interpretation of our seismic reflection data set, and Figure 7 presents the events sequentially in the form of a timeline.

The sliver fault seems to have been active since the Eocene and marked the eastern boundary of the continental crustal block. The accretionary wedge also started to grow in the Eocene (Figure 6a). The lowermost unit, Unit 1, was deposited conformably on top of the fore-arc basement, in a flat-lying setting, as suggested by the constant thickness of the unit within the fore-arc basin of all profiles used in this study.

This unit was then uplifted and tilted westward, along with the basement (Figure 6b). Either shortly after, or at roughly the same time, the back thrust initiated, that is, in early Miocene, similarly to the time of initiation of the back thrust in Mentawai [Mukti *et al.*, 2012]. The activity along the back thrust waned over time, as suggested by the thickening of the unit deformed by the back thrust, Unit 2.

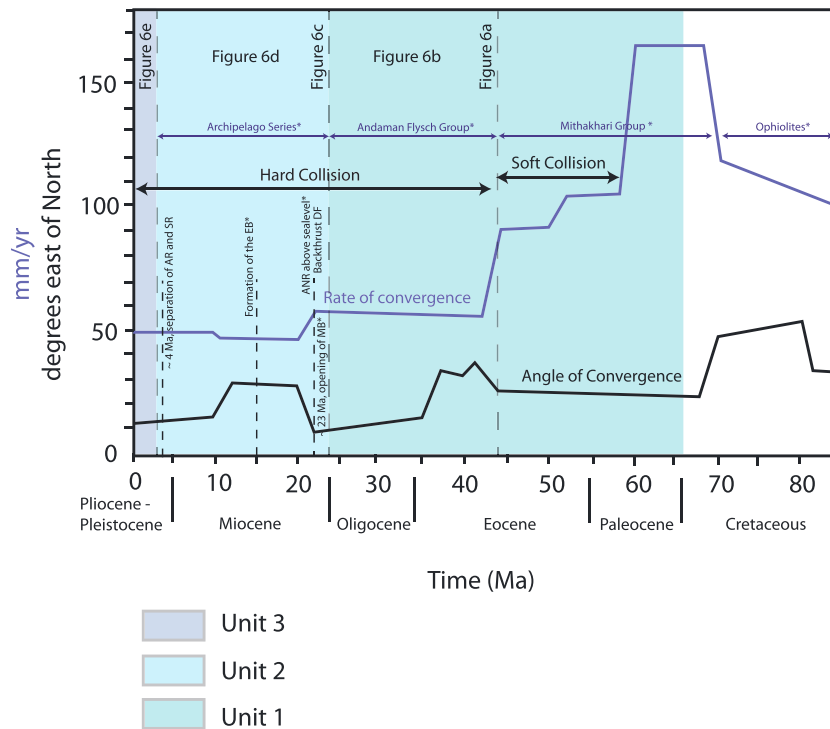


Figure 7. Timeline of evolution of the Andaman-Nicobar region. Adapted from *Lee and Lawver* [1995]. ANR = Andaman-Nicobar Ridge; DF = Diligent Fault; MB = Mergui Basin; EB = East Basin; and AR and SR = Alcock and Sewell Rises. Asterisks: for references in sections 2.3 and 4.

Significant uplift of the IB had occurred prior to the deposition of Unit 2, as indicated by the thinning of the unit and onlapping of the reflectors onto the top of Unit 1 (Figure 6c), but uplift continued with another episode during the deposition of Unit 2 (second subunit, Figure 6d). Significant amounts of compression continued to be accommodated in the fore arc and the inner accretionary wedge at this time, as suggested by the extensive folding of Unit 2 in a series of folds. Westward tilting and uplift of the eastern edge of the basin, as well as gradual submergence of the westward edge of the basin, thus seem to have occurred earlier than previously thought [Rodolfo, 1969; Curray, 2005]. Units deformed by the DF are also continuous to the west and can be seen at the base of the EMF basin, indicating that early subsidence along the EMF was coincident with compression along the back thrust. The shift of the sliver fault from the IB to its present position (ANF) likely occurred during this time, concurrently with the initial opening in the Andaman Sea, and thus also much earlier than ~4 Ma as suggested by Curray [2005], though it could also have happened later, during initiation of active spreading at the ASSC around 4 Ma ago.

The fact that the compressional folds are narrower and the DFZ thrust faults steeper in the south suggests that the fore-arc region is undergoing more compression in the south of the study area, despite opening at the ASSC in the north of the study area. Coincidentally, this area corresponds to the area where the NER indents the trench and the back thrust and strike-slip systems meet, east of the Nicobar Island. The sliver fault would thus act as a rigid boundary with respect to the fore arc, which is dominantly influenced by compression due to the subduction.

Most of the subsidence along the EMF occurred after the deposition of Unit 2, although some of the subsidence occurred concurrently (Figure 6d), as the top reflectors of Unit 2 can be traced continuously until the base of the EMF piggyback basin. Tensional features in the basin thus postdate the compressional structures that formed at the western edge of the basin.

Folded layers are overlain by a veneer of flat-lying recent sediments. Unit 3 was deposited in recent times (late Quaternary) and lies flat and conformably on top of Unit 2 (Figure 6e), indicating that very little uplift, if any, was occurring at the IB at the time of deposition of Unit 3. If this is the case, most of the uplift of the IB occurred earlier than suggested by Curray [2005], who had argued that most of the uplift of the IB occurred in recent times, in the last 4 Ma. More subsidence along the EMF occurred during that time,

however, as indicated by the thickness of the basin fill composed of recent sediments and the thickening of Unit 3 within that basin. The presence of multiple BSR-like events in the eastern portion of the EMF basin could be attributed to rapid tectonic movement or sedimentation in this basin, quicker than the gas hydrate system can reach a new equilibrium [Posewang and Mienert, 1999; Foucher *et al.*, 2002].

The fact that subsidence along the EMF and the thickness of Unit 3 are greater in the north of the study area could be due either to the closer proximity to the sediment source or to the larger size of the EMF basin. A closer proximity to the sediment source in the north is a more likely explanation, however, since the lows between the thrust sheets formed by the DFZ are filled with Unit 3 sediments in the northern profiles (e.g., Figure 2a) but not in the southern profiles (Figure 2b).

Contrasting patterns of deformation, particularly in the DFZ, between northern (PGS08-11 to PGS08-14) and southern profiles (PGS08-08 to PGS08-11) point to a change of regime at PGS08-11, which corresponds to where the NER begins to indent the margin (Figure 1a). This complexity could be related to the merging of the WAF back thrust system and the GSF sliver fault, east of the Nicobar Islands [Singh *et al.*, 2013].

Given that the uplift of the IB, activity along the BT, and the subsidence along the EMF seem to have occurred in distinct times, we propose that these events are related to different opening phases in the Andaman Sea (Figures 6c and 6d), since the IB and EMF are features unique to this segment of the margin, unlike the BT which is ubiquitous along Sumatra and into the Andaman Sea. Most of the uplift of the IB coincides with early stretching and rifting in the Andaman Sea (Figure 6c), while subsidence along the EMF seems to have occurred mostly around ~4 Ma, corresponding to the phase of active spreading (Figure 6d).

Two major events of plate geometry change are expressed in the subducted slab, as sharp changes in subduction angle [Khan and Chakraborty, 2005]. Those two anomalies in the subducting slab dip correspond to the 4–5 Ma and 11 Ma isochrons and are thus correlated with the well-established two-phase opening in the Andaman Sea. The 11 Ma event, recorded around 2°N, is correlated with early stretching and rifting in the Andaman Basin. The 4–5 Ma event, recorded around 7°N, is associated with active spreading in the Andaman Sea [Khan and Chakraborty, 2005]. The initial rifting phase seems to be strongly related to the obliquity due to the Indian collision. Tapponnier *et al.* [1982] argued that opening in the Mergui Basin and Andaman Sea had initiated as a direct kinematic consequence of the collision between India and Asia, which induced clockwise rotation and extrusion processes, activating major strike-slip fault systems in the region. The active spreading phase could be related to the late Miocene-Pliocene trench retreat and pull-apart trans-tension along the sliver fault system [Khan and Chakraborty, 2005]. Stretching in the overriding plate could have caused active fore-arc subsidence.

Our observations of the DF strongly resemble observations of the MFZ [Schlüter *et al.*, 2002; Mukti *et al.*, 2012]. Stratigraphy in the Mentawai fore-arc basin is divided into four megasequences based on drilling results [Hall *et al.*, 1993]. The basement, which could be Eocene-Cretaceous mélange of continental and oceanic material [Samuel *et al.*, 1997], is overlain by a thin unit of upper Eocene to Lower Oligocene sediments. The accretionary prism in Sumatra too is composed of ophiolite slices, interpreted to have been emplaced 90 Ma [Hall, 2012] and exposed in the fore-arc high islands [Samuel *et al.*, 1997]. The presence of extensional faults within the sediments of the fore-arc basin, active in the Plio-Pleistocene but short term as indicated by the lack of growth structures, is thought to be related to subsidence of the basin [Mukti *et al.*, 2012]. The Bengkulu Fault Zone [Mukti *et al.*, 2012] is related to a compressional phase of the subduction, which Hall [2012] has suggested to have initiated since at least the middle Eocene. Another phase of compression occurred during early and middle Miocene as indicated by the development of landward vergent back thrusts farther seaward in the Neogene accretionary wedge [Mukti *et al.*, 2012], corresponding to the initiation of the MFZ. These features indicate that the subduction process is the main control on the deformation within the South Sumatra fore-arc basin [Mukti *et al.*, 2012].

The fact that back thrusting initiated around the same time suggests that the Sumatra-Andaman subduction zone processes occurred on a regional scale and that slip is well partitioned between the trench and the sliver fault, along the Andaman-Nicobar segment of the subduction. Indeed, despite the high obliquity, the fore arc is still dominated by compression. Schlüter *et al.* [2002] have suggested similar plate tectonic regimes from SE Sumatra to NW Java by correlation of the major tectonic features in the fore arc. We suggest that the Andaman portion of the subduction was in a similar tectonic regime as well, except that its evolution is shaped by the interplay of the oblique subduction and opening in the Andaman Sea, which greatly affected deformation processes in the fore arc. Here while some motion on the DF could be strike slip in the surface,

the DF is primarily a back thrust but does not mark the boundary between continental crust in the east and fore-arc ridges in the west, like the WAF and MFZ off Sumatra [Singh *et al.*, 2013]. Instead, the EMF marks the boundary between continental crust in the fore arc and the Andaman-Nicobar Ridge. Uplift phases of the IB are related to opening phases in the Andaman Sea, with the sliver fault jumping from the eastern flank of the IB to its present-day position at the ANF.

Based on the observation of high reflectivity at the deep-rooted back thrusts in both the 2004 and the 2007 earthquake rupture areas, Singh *et al.* [2011] suggested that the BT may have ruptured coseismically. The migration of fluids from the mantle along these BT would be the cause of their enhanced reflectivity. Deep thrust earthquakes, down to 30 km, relocated using double difference [Pesicek *et al.*, 2010], are observed in the MFZ area. However, a lack of shallow seismicity is also noted. Slip along the BT within the Mentawai fore arc is suggested by a cluster of seismicity, with some thrust focal mechanisms [Collings *et al.*, 2012; Wiseman *et al.*, 2011; Mukti *et al.*, 2012]. Waning activity at the BT in the MFZ, suggested by a decrease of deformation within the sequential development of the BT as well as lack of shallow seismicity, seems to indicate that the risk of a large event along the BT is rather small. Similarly, no sign of present-day activity is observed at the DF. However, the concentration of BSRs, which are indicative of local fault and fracture networks and thus regional stresses, on either side of the DFZ and over the DFZ folds also point to the fact that the back thrusting system is the most active faulting feature in the fore-arc basin.

6. Conclusions

Our interpretation of a set of seismic reflection profiles across the Andaman-Nicobar fore-arc basin demonstrates that despite obliquity of subduction, the Andaman-Nicobar fore arc is dominated by compression, suggesting strong slip partitioning between strike-slip motion along the ANF and megathrust in the Andaman-Nicobar segment of the subduction zone. Additionally, while deformation and structure within the fore-arc basin are similar to the south, indicating the same tectonic regime operating all along the margin, the EMF and IB are tectonic elements unique to the Andaman-Nicobar portion of subduction. These structures are thus related to opening phases in the Andaman Sea. We show that compression and uplift of the IB had commenced much earlier than previously thought and the sliver fault jumped from the eastern flank of the IB to its present position at the ANF. The DF and EMF are probably not presently active.

Acknowledgments

We would like to thank Petroleum GeoServices for providing the Andaman Sea data. We would like to thank Greg Moore for his insight and very careful review of the paper. Seismic reflection data to support this article are from Petroleum GeoServices and cannot be released. The full uninterpreted images of the profiles used are provided in Figure 3. This is Institut de Physique du Globe de Paris contribution 3652.

References

- Berglar, K., C. Gaedicke, R. Lutz, D. Franke, and Y. S. Djajadihardja (2008), Neogene subsidence and stratigraphy of the Simeulue forearc basin, Northwest Sumatra, *Mar. Geol.*, *253*(1), 1–13.
- Bilham, R., R. Engdahl, N. Feldl, and S. P. Satyabala (2005), Partial and complete rupture of the Indo-Andaman plate boundary 1847–2004, *Seismol. Res. Lett.*, *76*(3), 299–311.
- Chakraborty, P. P., and T. Pal (2001), Anatomy of a forearc submarine fan: Upper Eocene—Oligocene Andaman Flysch Group, Andaman Islands, India, *Gondwana Res.*, *4*(3), 477–486.
- Chlieh, M., *et al.* (2007), Coseismic slip and afterslip of the great M_w 9.15 Sumatra–Andaman earthquake of 2004, *Bull. Seismol. Soc. Am.*, *97*(1A), S152–S173.
- Cochran, J. R. (2010), Morphology and tectonics of the Andaman Forearc, northeastern Indian Ocean, *Geophys. J. Int.*, *182*(2), 631–651.
- Collings, R., D. Lange, A. Rietbrock, F. Tilmann, D. Natawidjaja, B. Suwargadi, M. Miller, and J. Saul (2012), Structure and seismogenic properties of the Mentawai segment of the Sumatra subduction zone revealed by local earthquake traveltime tomography, *J. Geophys. Res.*, *117*, B01312, doi:10.1029/2011JB008469.
- Curray, J. R. (2005), Tectonics and history of the Andaman Sea region, *J. Asian Earth Sci.*, *25*(1), 187–232.
- Curray, J. R., and D. G. Moore (1974), Sedimentary and tectonic processes in the Bengal deep-sea fan and geosyncline, in *The Geology of Continental Margins*, pp. 617–627, Springer, Berlin.
- Curray, J. R., D. G. Moore, L. A. Lawver, F. J. Emmel, R. W. Raitt, M. Henry, and R. Kieckhefer (1979), Tectonics of the Andaman Sea and Burma, in *Geological and Geophysical Investigations of Continental Margins, Mem.*, vol. 29, edited by J. Watkins, L. Montadert, and P. W. Dickerson, pp. 189–198, Am. Assoc. Pet. Geol., Tulsa, Okla.
- Diament, M., H. Harjono, K. Karta, C. Deplus, D. Dahrin, M. T. Zen, M. Gérard, O. Lassel, A. Martin, and J. Malod (1992), Mentawai Fault Zone off Sumatra: A new key to the geodynamics of western Indonesia, *Geology*, *20*(3), 259–262.
- Dickinson, W. R., and D. R. Seely (1979), Structure and stratigraphy of forearc regions, *AAPG Bull.*, *63*(1), 2–31.
- Fitch, T. J. (1972), Plate convergence, transcurrent faults, and internal deformation adjacent to Southeast Asia and the western Pacific, *J. Geophys. Res.*, *77*(23), 4432–4460, doi:10.1029/JB077i023p04432.
- Flores, J. A., J. E. Johnson, A. E. Mejía-Molina, M. C. Álvarez, F. J. Sierro, S. D. Singh, S. Mahanti, and L. Giosan (2014), Sedimentation rates from calcareous nannofossil and planktonic foraminifera biostratigraphy in the Andaman Sea, northern Bay of Bengal, and Eastern Arabian Sea, *Mar. Pet. Geol.*, *58*, 425–437.
- Foucher, J. P., H. Nouzé, and P. Henry (2002), Observation and tentative interpretation of a double BSR on the Nankai slope, *Mar. Geol.*, *187*(1), 161–175.
- Fuller, C. W., S. D. Willett, and M. T. Brandon (2006), Formation of forearc basins and their influence on subduction zone earthquakes, *Geology*, *34*(2), 65–68.

- Gahalaut, V. K., B. Nagarajan, J. K. Catherine, and S. Kumar (2006), Constraints on 2004 Sumatra–Andaman earthquake rupture from GPS measurements in Andaman–Nicobar Islands, *Earth Planet. Sci. Lett.*, *242*(3), 365–374.
- Genrich, J. F., Y. Bock, R. McCaffrey, L. Prawirodirdjo, C. W. Stevens, S. S. O. Puntodewo, C. Subarya, and S. Wdowski (2000), Distribution of slip at the northern Sumatran fault system, *J. Geophys. Res.*, *105*(B12), 28,327–28,341, doi:10.1029/2000JB900158.
- Hall, D. M., B. A. Duff, M. C. Courbe, B. W. Seubert, M. Siahaan, and A. D. Wirabudi (1993), The southern fore-arc zone of Sumatra: Cainozoic basin-forming tectonism and hydrocarbon potential.
- Hall, R. (2012), Late Jurassic–Cenozoic reconstructions of the Indonesian region and the Indian Ocean, *Tectonophysics*, *570*, 1–41.
- Karig, D. E., S. Suparka, G. F. Moore, and P. E. Hehanussa (1979), Structure and Cenozoic evolution of the Sunda arc in the central Sumatra region, in *Geological and Geophysical Investigations of Continental Margins*, vol. 29, pp. 223–237, Am. Assoc. Pet. Geol., Tulsa, Okla.
- Khan, P. K., and P. P. Chakraborty (2005), Two-phase opening of Andaman Sea: A new seismotectonic insight, *Earth Planet. Sci. Lett.*, *229*(3), 259–271.
- Klootwijk, C. T., J. S. Gee, J. W. Peirce, G. M. Smith, and P. L. McFadden (1992), An early India-Asia contact: Paleomagnetic constraints from Ninetyeast Ridge, ODP Leg 121, *Geology*, *20*(5), 395–398.
- Larsen, J., D. W. Scholl, and R. von Huene (2002), Neotectonic deformation of the central Chile margin: Deepwater forearc basin formation in response to hot spot ridge and seamount subduction, *Tectonics*, *21*(5), 1038, doi:10.1029/2001TC901023.
- Lay, T., et al. (2005), The great Sumatra-Andaman earthquake of 26 December 2004, *Science*, *308*(5725), 1127–1133.
- Lee, T. Y., and L. A. Lawver (1995), Cenozoic plate reconstruction of Southeast Asia, *Tectonophysics*, *251*(1), 85–138.
- Marone, C. (1998), The effect of loading rate on static friction and the rate of fault healing during the earthquake cycle, *Nature*, *391*, 69–72, doi:10.1038/34157.
- Martin, K. M., S. P. Gulick, J. A. Austin, K. Berglar, D. Franke, and Udrek (2014), The West Andaman Fault: A complex strain-partitioning boundary at the seaward edge of the Aceh Basin, offshore Sumatra, *Tectonics*, *33*, 786–806, doi:10.1002/2013TC003475.
- McCaffrey, R. (1992), Oblique plate convergence, slip vectors, and forearc deformation, *J. Geophys. Res.*, *97*(B6), 8905–8915, doi:10.1029/92JB00483.
- Moeremans, R., S. C. Singh, M. Mukti, J. McArdle, and K. Johansen (2014), Seismic images of structural variations along the deformation front of the Andaman–Sumatra subduction zone: Implications for rupture propagation and tsunamigenesis, *Earth Planet. Sci. Lett.*, *386*, 75–85.
- Moore, G. F., J. R. Curry, D. G. Moore, and D. E. Karig (1980), Variations in geologic structure along the Sunda Fore Arc, northeastern Indian Ocean, in *The Tectonic and Geologic Evolution of Southeast Asian Seas and Islands. Part 1*, *Geophys. Monogr.*, vol. 23, edited by D. E. Hayes, pp. 145–160, AGU, Washington, D. C.
- Moore, G. F., J. R. Curry, and F. J. Emmel (1982), Sedimentation in the Sunda Trench and forearc region, *Geol. Soc. London Spec. Publ.*, *10*(1), 245–258.
- Morley, C. K., and A. Alvey (2015), Is spreading prolonged, episodic or incipient in the Andaman Sea? Evidence from deepwater sedimentation, *J. Asian Earth Sci.*, *98*, 446–456.
- Mukti, M., S. C. Singh, I. Deighton, N. D. Hananto, R. Moeremans, and H. Permana (2012), Structural evolution of backthrusting in the Mentawai Fault Zone, offshore Sumatran forearc, *Geochem. Geophys. Geosyst.*, *13*, Q12006, doi:10.1029/2012GC004199.
- Pal, T., P. P. Chakraborty, T. D. Gupta, and C. D. Singh (2003), Geodynamic evolution of the outer-arc–forearc belt in the Andaman Islands, the central part of the Burma–Java subduction complex, *Geol. Mag.*, *140*(03), 289–307.
- Paul, J., et al. (2001), The motion and active deformation of India, *Geophys. Res. Lett.*, *28*(4), 647–650, doi:10.1029/2000GL011832.
- Pesicek, J. D., C. H. Thurber, S. Widiyantoro, H. Zhang, H. R. DeShon, and E. R. Engdahl (2010), Sharpening the tomographic image of the subducting slab below Sumatra, the Andaman Islands and Burma, *Geophys. J. Int.*, *182*(1), 433–453.
- Posewang, J., and J. Mienert (1999), The enigma of double BSRs: Indicators for changes in the hydrate stability field?, *Geo Mar. Lett.*, *19*(1–2), 157–163.
- Prawirodirdjo, L., and Y. Bock (2004), Instantaneous global plate motion model from 12 years of continuous GPS observations, *J. Geophys. Res.*, *109*, B08405, doi:10.1029/2003JB002944.
- Rhie, J., D. Dreger, R. Bürgmann, and B. Romanowicz (2007), Slip of the 2004 Sumatra–Andaman earthquake from joint inversion of long-period global seismic waveforms and GPS static offsets, *Bull. Seismol. Soc. Am.*, *97*(1A), S115–S127.
- Rodolfo, K. S. (1969), Bathymetry and marine geology of the Andaman Basin, and tectonic implications for Southeast Asia, *Geol. Soc. Am. Bull.*, *80*(7), 1203–1230.
- Roy, T. K., and N. N. Chopra (1987), Wrench faulting in Andaman forearc basin, India, *Proc. Offshore Technol. Conf.*, *19*, 393–404.
- Ryan, H. F., A. E. Draut, K. Keranen, and D. W. Scholl (2012), Influence of the Amliia fracture zone on the evolution of the Aleutian Terrace forearc basin, central Aleutian subduction zone, *Geosphere*, *8*(6), 1254–1273.
- Samuel, M. A., N. A. Harbury, A. Bakri, F. T. Banner, and L. Hartono (1997), A new stratigraphy for the islands of the Sumatran Forearc, Indonesia, *J. Asian Earth Sci.*, *15*(4), 339–380.
- Schlüter, H. U., C. Gaedicke, H. A. Roeser, B. Schreckenberger, H. Meyer, C. Reichert, Y. Djajadihardja, and A. Prexl (2002), Tectonic features of the southern Sumatra–western Java forearc of Indonesia, *Tectonics*, *21*(5), 1047, doi:10.1029/2001TC901048.
- Sieh, K., and D. Natawidjaja (2000), Neotectonics of the Sumatran fault, Indonesia, *J. Geophys. Res.*, *105*(B12), 28,295–28,326, doi:10.1029/2000JB900120.
- Singh, S. C., N. D. Hananto, A. P. Chauhan, H. Permana, M. Denolle, A. Hendriyana, and D. Natawidjaja (2010), Evidence of active backthrusting at the NE margin of Mentawai Islands, SW Sumatra, *Geophys. J. Int.*, *180*(2), 703–714.
- Singh, S. C., N. D. Hananto, and A. P. S. Chauhan (2011), Enhanced reflectivity of backthrusts in the recent great Sumatran earthquake rupture zones, *Geophys. Res. Lett.*, *38*, L04302, doi:10.1029/2010GL046227.
- Singh, S. C., R. Moeremans, J. McArdle, and K. Johansen (2013), Seismic images of the sliver strike-slip fault and back thrust in the Andaman–Nicobar region, *J. Geophys. Res. Solid Earth*, *118*, 5208–5224, doi:10.1002/jgrb.50378.
- Stein, S., and E. A. Okal (2005), Seismology: Speed and size of the Sumatra earthquake, *Nature*, *434*(7033), 581–582.
- Tapponnier, P., G. Peltzer, A. Y. Le Dain, R. Armijo, and P. Cobbold (1982), Propagating extrusion tectonics in Asia: New insights from simple experiments with plasticine, *Geology*, *10*(12), 611–616.
- Vigny, C., A. Socquet, C. Rangin, N. Chamot-Rooke, M. Pubellier, M. N. Bouin, G. Bertrand, and M. Becker (2003), Present-day crustal deformation around Sagaing Fault, Myanmar, *J. Geophys. Res.*, *108*(B11), 2533, doi:10.1029/2002JB001999.
- Wiseman, K., P. Banerjee, K. Sieh, R. Bürgmann, and D. H. Natawidjaja (2011), Another potential source of destructive earthquakes and tsunami offshore of Sumatra, *Geophys. Res. Lett.*, *38*, L10311, doi:10.1029/2011GL047226.